Interband electron Raman scattering in a quantum wire in a transverse magnetic field

F. M. Hashimzade,[1] T. G. Ismailov,[2] B. H. Mehdiyev,[1] and S. T. Pavlov[3]

[1]*Institute of Physics, Azerbaijan Academy of Sciences, AZ 1143 Baku, Azerbaijan*
[2]*Baku State University, AZ 1073/1 Baku, Azerbaijan*
[3]*Facultad de Fisica de la UAZ, Apartado Postal C-580, 98060 Zacatecas, Zac., Mexico*
and P. N. Lebedev Physical Institute, Russian Academy of Sciences, 119991 Moscow, Russia

Electron Raman scattering (ERS) is investigated in a parabolic semiconductor quantum wire in a transverse magnetic field neglected by phonon-assisted transitions. The ERS cross section is calculated as a function of a frequency shift and magnetic field. The process involves an interband electronic transition and an intraband transition between quantized subbands. We analyze the differential cross section for different scattering configurations. We study selection rules for the processes. Some singularities in the Raman spectra are found and interpreted. The scattering spectrum shows density-of-states peaks and interband matrix elements maxima and a strong resonance when the scattered frequency equals the "hybrid" frequency or confinement frequency depending on the light polarization. Numerical results are presented for a GaAs/AlGaAs quantum wire.

I. INTRODUCTION

Low-dimensional semiconductor systems, quantum wires in particular, have attracted considerable attention because of their novel physical properties and application potential. In recent years a number of innovative techniques have been developed to grow or to fabricate and to study experimentally a variety of quantum wire structures having different geometries and potentials. Many recent experimental and theoretical studies have been performed on quantum wires subjected to a transverse magnetic field.[1–7] Electronic properties of quantum wells in a transverse magnetic field have been investigated in Refs. 8 and 9. The subband dispersion and magnetoabsorption have been studied for rectangular quantum wires in Ref. 10.

A magnetic field perpendicular to the wire axis (a "free-electron" direction) can change significantly the electronic states of a semiconductor quantum wire.

Electron Raman scattering (ERS) seems to be a useful technique, providing direct information on the energy band structure and optical properties of the investigated systems.[11–13] In particular, the electronic structure of semiconductor materials and nanostructures can be thoroughly investigated considering different polarizations for the incident and emitted radiation.[14] The differential cross section, in the general case, usually shows singularities related to interband and intraband transitions. This latter result strongly depends on the scattering configurations: the structure of singularities varies when photon polarizations change. This feature of ERS allows us to determine the subband structure of the system by a direct inspection of singularity positions in the spectra. For bulk semiconductors ERS has been studied in the presence of external magnetic and electric fields.[15–17] In the case of a quantum well preliminary results were reported in Ref. 18.

Raman scattering in low-dimensional semiconductor systems has been the subject of many theoretical and experimental investigations.[19,20] Interband ERS processes can be qualitatively described in the following way: absorption of a photon of the incident radiation field creates a virtual electron-hole pair (EHP) in an intermediate crystal state by means of an electron interband transition involving the crystal valence and conduction bands. An electron in the conduction band is subject to a second intraband transition with emission of a secondary radiation photon. Therefore, in the final state we have a real EHP in the crystal and a photon of the secondary radiation. The influence of external fields on such processes for bulk semiconductors is investigated in Refs. 16 and 17.

In this work we present a systematic study of the interband ERS in a direct band gap semiconducting parabolic quantum wire in a transverse magnetic field. In these systems, due to electron confinement and magnetic field, the conduction (valence) band is split in a subband system and transitions between them determine ERS processes. Numerical results for the ERS differential cross section are presented for a GaAs/AlGaAs quantum wire. This artical is organized as follows. In Sec. II the energy spectrum and wave functions for a quantum wire with parabolic confinement potential in a transverse magnetic field are given. In Sec. III we present the general relations needed for our calculations of the ERS differential cross section. Section IV is devoted to calculations of ERS differential cross sections. Finally, Sec. V is concerned with a discussion of the obtained results.

II. WAVE FUNCTIONS AND ENERGY SPECTRUM

We consider a quantum wire aligned along the y axis with a transverse magnetic field $\mathbf{H}=\mathbf{H}(0,0,H)$ applied along the z axis. The quantum wire is characterized by parabolic confinements in the (x,z) plane. The effective mass Schrödinger equation for an electron in a conduction band is

$$\left[\frac{1}{2m_e}\left(\mathbf{p}+\frac{e}{c}\mathbf{A}\right)^2+\frac{1}{2}m_e\omega_{0e}^2(x^2+z^2)\right]\psi_e(x,y,z)=E_e\psi_e(x,y,z),$$
$$(1)$$

where $\mathbf{A}=\mathbf{A}(0,xH,0)$ is the vector potential in the Landau gauge, ω_{0e} characterizes the parabolic potential of a quantum wire for electrons in a conduction band, and m_e and $-e$ are the electron effective mass and charge, respectively. We look for the solution in the form

$$\psi_e(x,y,z)=\varphi(x)\,\eta(z)e^{ip_{y,e}y/\hbar},$$

where $p_{y,e}=\hbar k_{y,e}$ is the quasimomentum of an electron.

Shifting the origin of coordinates and separating the variables in the usual way we obtain the eigenfunctions and eigenvalues of the Schrödinger equation (1):

$$\psi_{N_{1e},N_{2e},k_{y,e}}=\varphi_{N_{1e}}\left(\frac{x-x_{0e}}{\tilde{L}_e}\right)\eta_{N_{2e}}\left(\frac{z}{L_e}\right)e^{ik_{y,e}y},\qquad(2)$$

$$E_e=(N_{1e}+1/2)\hbar\tilde{\omega}_e+(N_{2e}+1/2)\hbar\omega_{0e}+\frac{\hbar^2k_{y,e}^2}{2m_e}\left(\frac{\omega_{0e}}{\tilde{\omega}_e}\right)^2.$$
$$(3)$$

The wave functions and energy eigenvalues for electrons in valence band are as follows:

$$\psi_{N_{1h},N_{2h},k_{y,h}}=\varphi_{N_{1h}}\left(\frac{x-x_{0h}}{\tilde{L}_e}\right)\eta_{N_{2h}}\left(\frac{z}{L_h}\right)e^{ik_{y,h}y},\qquad(4)$$

$$E_h=-E_g-(N_{1h}+1/2)\hbar\tilde{\omega}_h-(N_{2h}+1/2)\hbar\omega_{0h}$$
$$-\frac{\hbar^2k_{y,h}^2}{2m_h}\left(\frac{\omega_{0h}}{\tilde{\omega}_h}\right)^2,\qquad(5)$$

where E_g is the energy gap between the valence and conduction bands in the absence of an external magnetic field and ω_{0h} is the oscillator frequency of the parabolic potential for electrons in the valence band. In Eqs. (2)–(5),

$$\tilde{\omega}_{e,h}=\sqrt{\omega_{0e(h)}^2+\omega_{e(h)}^2}\qquad(6)$$

is the "hybrid" frequency. The subscripts e and h denote conduction and valence bands, respectively,

$$\omega_{e(h)}=\frac{eH}{m_{e(h)}c}\qquad(7)$$

is the cyclotron frequency, $m_{e(h)}$ is the effective mass, and

$$x_{0e(h)}=\frac{\hbar\omega_{e(h)}}{m_{e(h)}\tilde{\omega}_{e(h)}^2}k_{ye(h)}\qquad(8)$$

is the oscillator center.

The full energy spectrum in Eqs. (2)–(5) is governed by the quantum numbers $N_{1e(h)}$, $N_{2e(h)}$, and $k_{ye(h)}$:

$$\varphi_{N_{1e(h)}}\left(\frac{x-x_{0e(h)}}{\tilde{L}_{e(h)}}\right)$$
$$=\left(\frac{1}{\pi\tilde{L}_{e(h)}^2}\right)^{1/4}\frac{1}{\sqrt{2^{N_{1e(h)}}N_{1e(h)}!}}$$
$$\times\exp\left(-\frac{(x-x_{0e(h)})^2}{2\tilde{L}_e^2}\right)H_{N_{1e(h)}}\left(\frac{x-x_{0e(h)}}{\tilde{L}_{e(h)}}\right),\quad(9)$$

$$\eta_{N_{2e(h)}}\left(\frac{z}{L_{e(h)}}\right)=\left(\frac{1}{\pi L_{e(h)}^2}\right)^{1/4}\frac{1}{\sqrt{2^{N_{2e(h)}}N_{2e(h)}!}}$$
$$\times\exp\left(-\frac{z^2}{2L_{e(h)}^2}\right)H_{N_{2e(h)}}\left(\frac{z}{L_{e(h)}}\right),\quad(10)$$

where the parameters

$$\tilde{L}_{e(h)}=\sqrt{\frac{\hbar}{m_{e(h)}\tilde{\omega}_{e(h)}}},\quad L_{e(h)}=\sqrt{\frac{\hbar}{m_{e(h)}\omega_{0e(h)}}}\qquad(11)$$

are the units of length; $H_n(\xi)$ is the Hermitian polynomial.

III. PRELIMINARY RELATIONS

The general expression for the ERS differential cross section is given by[16,18]

$$\frac{d^2\sigma}{d\Omega d\nu_s}=\frac{V^2\nu_s^2n(\nu_s)}{8\pi^3c^4n(\nu_l)}W(\nu_s,\mathbf{e}_s),\qquad(12)$$

where c is the light velocity in vacuum, $n(\nu)$ is refraction index as a function of the radiation frequency, $\mathbf{e}_s$ is the (unit) polarization vector for the secondary radiation field, V is the normalization volume, ν_s is the secondary radiation frequency, and ν_l is the frequency of the incident radiation. $W(\nu_s,\mathbf{e}_s)$ is the transition rate calculated according to

$$W(\nu_s,\mathbf{e}_s)=\frac{2\pi}{\hbar}\sum_f|M_e+M_h|^2\delta(E_f-E_i),\qquad(13)$$

where

$$M_j=\sum_a\frac{\langle f|\hat{H}_{js}|a\rangle\langle a|\hat{H}_l|i\rangle}{E_i-E_a}+\sum_b\frac{\langle f|\hat{H}_l|b\rangle\langle b|\hat{H}_{js}|i\rangle}{E_i-E_b}.\qquad(14)$$

In Eq. (14), $j=e,h$ are for the cases of electrons or holes, respectively, and $|i\rangle$ and $|f\rangle$ denote initial and final states of the system with their corresponding energies E_i and E_f. $|a\rangle$ and $|b\rangle$ are intermediate states with energies E_a and E_b.

The operator $\hat{H}_l$ is of the form

$$\hat{H}_l=\frac{|e|}{m_0}\sqrt{\frac{2\pi\hbar}{V\nu_l}}\mathbf{e}_l\cdot\hat{\mathbf{p}},\quad\hat{\mathbf{p}}=-i\hbar\nabla,\qquad(15)$$

where m_0 is the free-electron mass. This operator describes the interaction with the incident radiation field in the dipole approximation. The interaction with the secondary-radiation field is described by the operator

$$\hat{H}_{js}=\frac{|e|}{m_j}\sqrt{\frac{2\pi\hbar}{V\nu_s}}\mathbf{e}_s\cdot\hat{\mathbf{p}},\quad j=e,h.\qquad(16)$$

This Hamiltonian describes the photon emission by the electron (hole) after transitions between conduction (valence) subbands of the system. In Eq. (14) the intermediate states $|a\rangle$ represent an EHP in a virtual state (after absorption of the incident photon), while the states $|b\rangle$ are related to the "interference diagrams."[16,18] This latter term involves a negligible contribution whenever the energy gap E_g is large enough (for instance, this is the case for GaAs) and will not be considered in the present work.

We established that the processes of ERS given in the following are possible.

(a) *The interband ERS process with the intermediate state in the conduction band.* First, an incident light quantum is being absorbed creating an electron-hole pair between the state (N_{1h}, N_{2h}) in the valence band and the state (N'_{1e}, N'_{2e}) in the conduction band. Second, a scattered photon is emitted due to an electronic transition from the state (N'_{1e}, N'_{2e}) to the state (N_{1e}, N_{2e}) in the conduction band. The Raman shift $\hbar\nu = \hbar(\nu_l - \nu_s)$ is equal to the excitation energy of the electron-hole pair created in the scattering process.

(b) *The interband ERS process with the intermediate state in the valence band.* Two electrons take part in the process. After the absorption of an incident photon the first electron from the state (N'_{1h}, N'_{2h}) in the valence band is lifted to the state (N_{1e}, N_{2e}). The second electron from the state (N_{1h}, N_{2h}) falls to the vacant state in the (N'_{1h}, N'_{2h}) subband. The real transition corresponds to a transition from the state (N_{1h}, N_{2h}) to the state (N_{1e}, N_{2e}).

In the initial state $|i\rangle$ we have an incident radiation photon with frequency ν_l, while the conduction band is empty and the valence band completely occupied by electrons. We neglect by all the transitions assisted by phonons.

The initial state energy is

$$E_i = \hbar\nu_l. \qquad (17)$$

The final state of the process consists of an EHP in a real state and a scattered light with energy $\hbar\nu_s$. Thus,

$$E_f = \hbar\nu_s + E_{N_{1h}} + E_{N_{2h}} + E_{N_{1e}} + E_{N_{2e}} + E_g$$
$$+ \frac{\hbar^2 k_{ye}^2}{2m_e}\left(\frac{\omega_{0e}}{\tilde{\omega}_e}\right)^2 + \frac{\hbar^2 k_{yh}^2}{2m_h}\left(\frac{\omega_{0h}}{\tilde{\omega}_h}\right)^2, \qquad (18)$$

where

$$E_{N_{1e(h)}} = (N_{1e(h)} + 1/2)\hbar\tilde{\omega}_{e(h)},$$

$$E_{N_{2e(h)}} = (N_{2e(h)} + 1/2)\hbar\omega_{0e(h)}. \qquad (19)$$

For the electron intermediate states $|a\rangle$ the energies E_a are easily obtained from the above discussion:

$$E_i - E_a = -E_g - E_{N_{1h}} - E_{N_{2h}} - E_{N'_{1e}} - E_{N'_{2e}}$$
$$- \frac{\hbar^2 k_{ye}^2}{2m_e}\left(\frac{\omega_{0e}}{\tilde{\omega}_e}\right)^2 - \frac{\hbar^2 k_{yh}^2}{2m_h}\left(\frac{\omega_{0h}}{\tilde{\omega}_h}\right)^2 + \hbar\nu_l. \qquad (20)$$

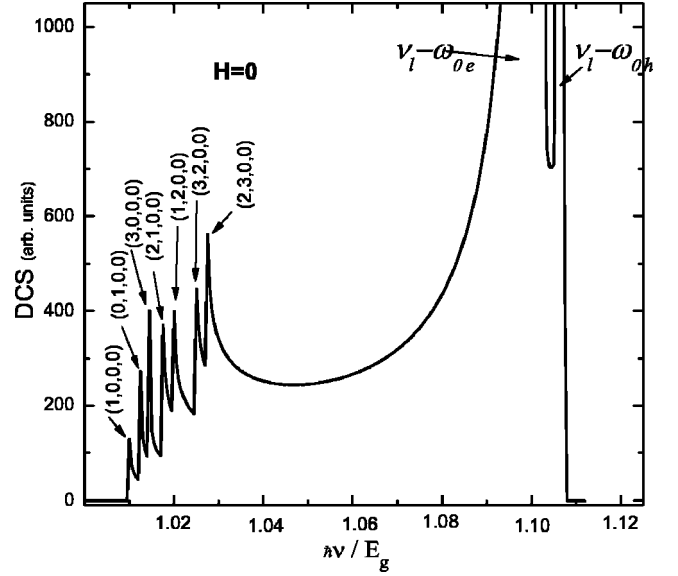Similar expressions can be written for the hole intermediate-state energies.

FIG. 1. The Raman spectra of the parabolic quantum wire in the X scattering configuration for $H=0$. The diameter d of the quantum wire is 2000 Å. The incident radiation frequency $\hbar\nu_0 = 1.68$ eV. The positions of the singularities are defined by Eqs. (A22) and (A23). Resonant electron-hole transitions are indicated by N_{1h}, N_{1e}, N_{2h}, N_{2e}.

IV. RESULTS AND DISCUSSION

In the following we present detailed numerical calculations of the differential cross section of a GaAs/AlGaAs parabolic quantum wire in the presence of uniform magnetic field as a function of $\hbar\nu/E_g$. The physical parameters used in our expressions are $E_g = 1.5177$ eV, $m_e = 0.0665m_0$, and $m_h = 0.45m_0$ (the heavy-hole band). Taking the ratio 60:40 for the band-edge discontinuity,[20,21] the conduction and valence barrier heights are taken to be $\Delta_e = 255$ meV and $\Delta_h = 170$ meV. The oscillation frequencies ω_{0e} and ω_{0h} of the parabolic quantum wire are determined as
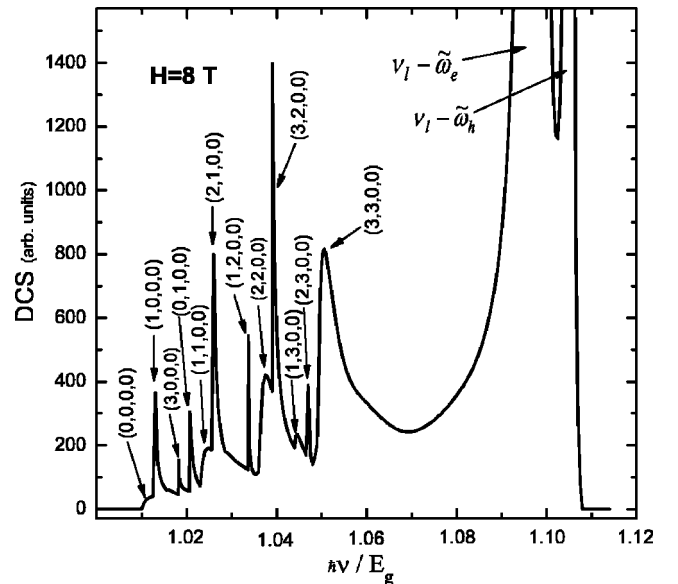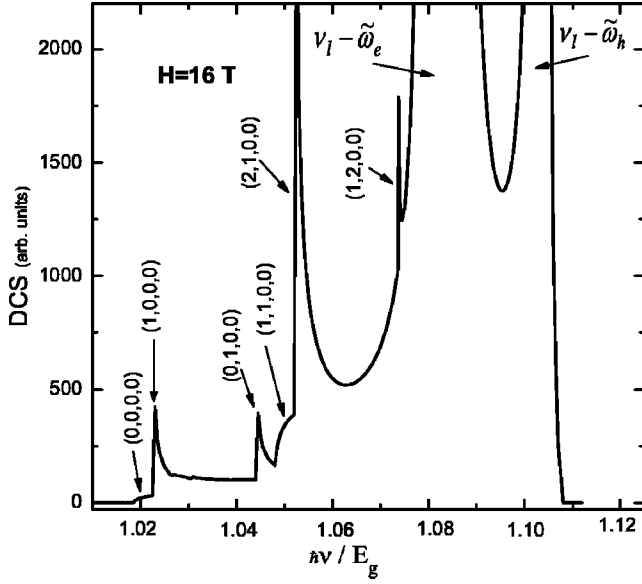

FIG. 2. Same that in Fig. 1 for $H=8$ T.

FIG. 3. Same that in Fig. 1 for $H=16$ T.

$$\omega_{0e(h)} = \frac{2}{d}\sqrt{\frac{2\Delta_{e(h)}}{m_{e(h)}}},$$

where d is the quantum wire diameter.

In Figs. 1–3 we show the Raman spectra of the parabolic quantum wire in the X scattering configuration for different magnetic fields. The diameter d of the quantum wire is 2000 Å. The incident radiation frequency $\hbar\nu_l = 1.68$ eV. The positions of the singularities are defined by Eqs. (A22)–(A24).

Figures 4 and 5 show the Raman spectra for the Z scattering configuration for the magnetic fields $H=8$ T and $H=16$ T. Other parameters coincide with those of Figs. 1–3.
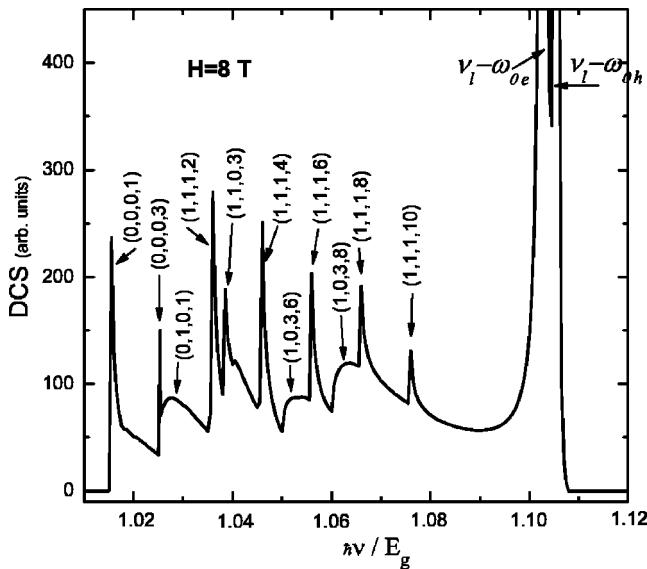
FIG. 4. The Raman spectra for the Z scattering configuration for the magnetic fields $H=8$ T. Other parameters coincide with those of Figs. 1–3.
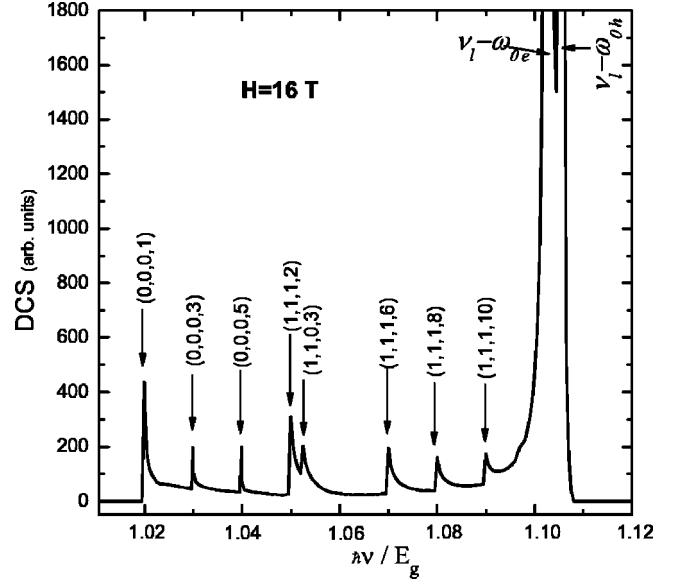
FIG. 5. The Raman spectra for the Z scattering configuration for the magnetic fields $H=16$ T. Other parameters coincide with those of Figs. 1–3.

The structure of the differential cross section, as given in the figures, provides a transparent understanding of the energy subband structure of the parabolic quantum wire in a transverse magnetic field.

In the present work we have applied a simplified model for the electronic structure of the system. In a more realistic case we should consider the real band structure using a calculation model like that of the Luttinger-Kohn or Kane model. The above-mentioned assumptions would lead to better results, but entail more complicated calculations. However, within the limits of our simple model we are able to take into account the essential physical properties of the discussed problem. The fundamental features of the differential cross section, as described in our work, should not change very much in real quantum wire case.

It can be easily proved that the singular peak in the differential cross section will be present irrespective of the model used for the subband structure and may be determined for the values of $\hbar\nu_s$ equal to the energy difference between two subbands $\hbar\nu_s = \hbar\nu_l - \hbar\nu = E^e_\alpha - E^e_\beta$, where $E^e_\alpha > E^e_\beta$ are electron energies in the subbands, respectively. At present there is a lack of experimental work on this type of the ERS. Our major aim in performing these calculations is to stimulate experimental research in this direction.[22]

APPENDIX: CALCULATION OF THE RAMAN SCATTERING CROSS SECTION

The matrix elements of the intraband transitions may be written as

$$\frac{|e|}{m_e}\sqrt{\frac{2\pi\hbar}{V\nu_s}}\langle N_{1e},N_{2e},k_{ye}|\mathbf{e_s p}|N'_{1e}N'_{2e},k'_{ye}\rangle$$

$$=\frac{|e|}{m_e}\sqrt{\frac{2\pi\hbar}{V\nu_s}}[\langle N_{1e},N_{2e},k_{ye}|e_{sx}p_x|N'_{1e}N'_{2e},k'_{ye}\rangle$$

$$+\langle N_{1e},N_{2e},k_{ye}|e_{sy}p_y|N'_{1e}N'_{2e},k'_{ye}\rangle$$

$$+\langle N_{1e},N_{2e},k_{ye}|e_{sz}p_z|N'_{1e}N'_{2e},k'_{ye}\rangle],\tag{A1}$$

where

$$\langle N_{1e},N_{2e},k_{ye}|e_{sx}p_x|N'_{1e}N'_{2e},k'_{ye}\rangle$$

$$=-\frac{i\hbar}{\widetilde{L}_e}e_{sx}\delta_{N'_{2e},N_{2e}}\left[\sqrt{\frac{N_{1e}}{2}}\delta_{N'_{1e},N_{1e}-1}\right.$$

$$\left.-\sqrt{\frac{N_{1e}+1}{2}}\delta_{N'_{1e},N_{1e}+1}\right]\delta_{k_{ye},k'_{ye}},\tag{A2}$$

$$\langle N_{1e},N_{2e},k_{ye}|e_{sy}p_y|N'_{1e}N'_{2e},k'_{ye}\rangle=\hbar k'_{ye}e_{sy}\delta_{N'_{2e},N_{2e}}\delta_{N'_{2e},N_{2e}}\delta_{k_{ye},k'_{ye}},\tag{A3}$$

$$\langle N_{1e},N_{2e},k_{ye}|e_{sz}p_z|N'_{1e}N'_{2e},k'_{ye}\rangle$$

$$=-\frac{i\hbar}{L_e}e_{sz}\delta_{N'_{1e},N_{1e}}\left[\sqrt{\frac{N_{2e}}{2}}\delta_{N'_{2e},N_{2e}-1}\right.$$

$$\left.-\sqrt{\frac{N_{2e}+1}{2}}\delta_{N'_{2e},N_{2e}+1}\right]\delta_{k_{ye},k'_{ye}}.\tag{A4}$$

A similar expression can be written for the interband ERS process with the intermediate state in the valence band:

$$\frac{|e|}{m_h}\sqrt{\frac{2\pi\hbar}{V\nu_s}}\langle N'_{1h},N'_{2h},k'_{yh}|\mathbf{e_s p}|N_{1h},N_{2h},k_{yh}\rangle$$

$$=\frac{|e|}{m_h}\sqrt{\frac{2\pi\hbar}{V\nu_s}}[\langle N'_{1h},N'_{2h},k'_{yh}|e_{sx}p_x|N_{1h},N_{2h},k_{yh}\rangle$$

$$+\langle N'_{1h},N'_{2h},k'_{yh}|e_{sy}p_y|N_{1h},N_{2h},k_{yh}\rangle$$

$$+\langle N'_{1h},N'_{2h},k'_{yh}|e_{sz}p_z|N_{1h},N_{2h},k_{yh}\rangle],\tag{A5}$$

where

$$\langle N'_{1h},N'_{2h},k'_{yh}|e_{sx}p_x|N_{1h},N_{2h},k_{yh}\rangle$$

$$=-\frac{i\hbar}{\widetilde{L}_h}e_{sx}\delta_{N_{2h},N'_{2h}}\left[\sqrt{\frac{N_{1h}+1}{2}}\delta_{N_{1h},N'_{1h}-1}\right.$$

$$\left.-\sqrt{\frac{N_{1h}}{2}}\delta_{N_{1h},N'_{1h}+1}\right]\delta_{k_{yh},k'_{yh}},\tag{A6}$$

$$\langle N'_{1h},N'_{2h},k'_{yh}|e_{sy}p_y|N_{1h},N_{2h},k_{yh}\rangle$$

$$=\hbar k_{yh}e_{sy}\delta_{N_{2h},N'_{2h}}\delta_{N_{1h},N'_{1h}}\delta_{k_{yh},k'_{yh}},\tag{A7}$$

and

$$\langle N'_{1h},N'_{2h},k'_{yh}|e_{sz}p_z|N_{1h},N_{2h},k_{yh}\rangle$$

$$=-\frac{i\hbar}{L_h}e_{sz}\delta_{N_{1h},N'_{1h}}\left[\sqrt{\frac{N_{2h}+1}{2}}\delta_{N_{2h},N'_{2h}-1}\right.$$

$$\left.-\sqrt{\frac{N_{2h}}{2}}\delta_{N_{2h},N'_{2h}+1}\right]\delta_{k_{yh},k'_{yh}}.\tag{A8}$$

If we consider allowed electron transitions between conduction and valence bands, the interband matrix element in the envelope function approximation may be written as

$$\langle a|\hat{H}_l|i\rangle=\frac{|e|}{m_0}\sqrt{\frac{2\pi\hbar}{V\nu_l}}(\mathbf{p}_{cv}\mathbf{e}_l)$$

$$\times\begin{cases}I_{N_{1h},N'_{1e}}(k_y)J_{N_{2h},N'_{2e}}\delta_{k_{yh},k'_{ye}},&j=e,\\ I_{N'_{1h},N_{1e}}(k_y)J_{N'_{2h},N_{2e}}\delta_{k'_{yh},k_{ye}},&j=h,\end{cases}\tag{A9}$$

where $\mathbf{p}_{cv}$ is the momentum matrix element between the valence and conduction bands (evaluated at $\mathbf{k}=0$).

We find that the matrix elements (A2)–(A9) vanish unless the following selection rule is satisfied:

$$k_{ye}=k_{yh}=k'_{ye}=k'_{yh}=k_y.\tag{A10}$$

The EHP does not change its total momentum during absorption or emission of a photon (a photon momentum is neglected). It may be obtained that

$$I_{N_{1h},N'_{1e}}(k_y)=\left(\frac{1}{\pi}\right)^{1/2}\left(\frac{1}{\widetilde{L}_h\widetilde{L}_e}\right)^{1/2}\frac{N_{1h}!N'_{1e}!}{\sqrt{2^{N_{1h}+N'_{1e}}N_{1h}!N'_{1e}!}}$$

$$\times\sum_{k=0}^{[N_{1h}/2]}\sum_{k=0}^{[N'_{1e}/2]}\frac{(-1)^{k+j}2^{N_{1h}+N'_{1e}-2k-2j}}{k!j!(N_{1h}-2k)!(N'_{1e}-2j)!}$$

$$\times\left(\frac{1}{\widetilde{L}_e}\right)^{N'_{1e}-2j}\left(\frac{1}{\widetilde{L}_h}\right)^{N_{1h}-2k}$$

$$\times\sum_{\mu=0}^{N_{1h}-2k}\frac{(N_{1h}-2k)!}{\mu!(N_{1h}-2k-\mu)!}(x_{0e}-x_{0h})^{N_{1h}-2k-\mu}$$

$$\times\sum_{\nu=0}^{N'_{1e}-2j+\mu}\frac{(N'_{1e}-2j+\mu)!}{\nu!(N'_{1e}-2j+\mu-\nu)!}[(-1)^{\nu}+1]$$

$$\times\exp\left(\frac{-(x_{0e}-x_{0h})^2}{2(\widetilde{L}_e^2+\widetilde{L}_h^2)}\right)\frac{1}{2}\left(\frac{\widetilde{L}_e^2+\widetilde{L}_h^2}{2\widetilde{L}_e^2\widetilde{L}_h^2}\right)^{-(\nu+1)/2}$$

$$\times\Gamma\left(\frac{\nu+1}{2}\right)\left(-\frac{\widetilde{L}_e^2(x_{0e}-x_{0h})}{\widetilde{L}_e^2+\widetilde{L}_h^2}\right)^{N'_{1e}-2j+\mu-\nu}\tag{A11}$$

and

$$J_{N_{2h},N'_{2e}} = \left(\frac{1}{\pi}\right)^{1/2} \left(\frac{1}{L_h L_e}\right)^{1/2} \sqrt{\frac{N_{2h}! N'_{2e}!}{2^{N_{2h}+N'_{2e}}}}$$

$$\times \sum_{\alpha=0}^{[N'_{2e}/2]} \sum_{\beta=0}^{[N_{2h}/2]} \frac{(-1)^{\alpha+\beta} 2^{N'_{2e}-2\alpha+N_{2h}-2\beta}}{\alpha! \beta! (N'_{2e}-2\alpha)! (N_{2h}-2\beta)!}$$

$$\times \left(\frac{1}{L_e}\right)^{N'_{2e}-2\alpha} \left(\frac{1}{L_h}\right)^{N_{2h}-2\beta} [(-1)^{N'_{2e}+N_{2h}-2\alpha-2\beta}+1]$$

$$\times \frac{\Gamma\left(\dfrac{N'_{2e}+N_{2h}-2\alpha-2\beta+1}{2}\right)}{2\left(\dfrac{\sqrt{L_e^2+L_h^2}}{\sqrt{2}L_h L_e}\right)^{N'_{2e}+N_{2h}-2\alpha-2\beta+1}}. \tag{A12}$$

An expression analogous to Eqs. (A11) and (A12) holds for $I_{N'_{1h},N_{1e}}(k_y)$ and $J_{N'_{2h},N_{2e}}$ after making the replacements $N_{1h} \to N'_{1h}$ and $N_{2h} \to N'_{2h}$.

Performing the summation over k_y in Eq. (13) we obtain the ERS differential cross section:

$$\frac{d^2\sigma}{d\Omega d\nu_s} = \left(\frac{d^2\sigma}{d\Omega d\nu_s}\right)_{e_{sx}} + \left(\frac{d^2\sigma}{d\Omega d\nu_s}\right)_{e_{sy}} + \left(\frac{d^2\sigma}{d\Omega d\nu_s}\right)_{e_{sz}}, \tag{A13}$$

where

$$\left(\frac{d^2\sigma}{d\Omega d\nu_s}\right)_{e_{sx}} = \frac{\sigma_0}{\widetilde{L}_e^2} \frac{\nu_l - \nu}{\nu_l}$$

$$\times \sum_{N_{1e},N_{2e},N_{1h},N_{2h}} \left[\sum_{N'_{1e},N'_{2e},N'_{1h},N'_{2h}} \left\{ \frac{\beta}{A(\nu)} \delta_{N_{2e},N'_{2e}} \right. \right.$$

$$\times [\sqrt{N_{1e}/2}\, \delta_{N'_{1e},N_{1e}-1} - \sqrt{(N_{1e}+1)/2}\, \delta_{N'_{1e},N_{1e}+1}]$$

$$\times I_{N_{1h},N'_{1e}}(k_y(\nu)) J_{N_{2h},N'_{2e}} + \frac{\gamma(H)}{B(\nu)} \delta_{N_{2h},N'_{2h}}$$

$$\times I_{N'_{1h},N_{1e}}(k_y(\nu)) J_{N'_{2h},N_{2e}} \left(\sqrt{\frac{N_{1h}+1}{2}}\, \delta_{N_{1h},N'_{1h}-1} \right.$$

$$\left. \left. \left. - \sqrt{\frac{N_{1h}}{2}}\, \delta_{N_{1h},N'_{1h}+1} \right) \right\} \right]^2$$

$$\times \left(\frac{E_g}{\hbar\nu - E_{N_{1e}} - E_{N_{1h}} - E_{N_{2e}} - E_{N_{2h}} - E_g} \right)^{1/2}$$

$$\times |\mathbf{e}_s \cdot \mathbf{X}|^2 \tag{A14}$$

and

$$\left(\frac{d^2\sigma}{d\Omega d\nu_s}\right)_{e_{sy}} = \frac{\sigma_0}{L_e^2} \frac{\nu_l - \nu}{\nu_l}$$

$$\times \sum_{N_{1e},N_{2e},N_{1h},N_{2h}} \left[\sum_{N'_{1e},N'_{2e},N'_{1h},N'_{2h}} \left\{ \frac{\beta}{A(\nu)} \right. \right.$$

$$\times I_{N_{1h},N'_{1e}}(k_y(\nu)) J_{N_{2h},N'_{2e}} \delta_{N_{2e},N'_{2e}} \delta_{N_{1e},N'_{1e}}$$

$$+ \frac{1}{B(\nu)} I_{N'_{1h},N_{1e}}(k_y(\nu)) J_{N'_{2h},N_{2e}} \delta_{N_{2h},N'_{2h}} \delta_{N_{1h},N'_{1h}} \Big\} \Big]^2$$

$$\times \left(\frac{E_g}{\hbar\nu - E_{N_{1e}} - E_{N_{1h}} - E_{N_{2e}} - E_{N_{2h}} - E_g} \right)^{1/2}$$

$$\times (k_y(\nu) L_e)^2 |\mathbf{e}_s \cdot \mathbf{Y}|^2, \tag{A15}$$

$$\left(\frac{d^2\sigma}{d\Omega d\nu_s}\right)_{e_{sz}} = \frac{\sigma_0}{L_e} \frac{\nu_l - \nu}{\nu_l}$$

$$\times \sum_{N_{1e},N_{2e},N_{1h},N_{2h}} \left[\sum_{N'_{1e},N'_{2e},N'_{1h},N'_{2h}} \left\{ \frac{\beta}{A(\nu)} \delta_{N_{2e},N'_{2e}} \right. \right.$$

$$\times [\sqrt{N_{2e}/2}\, \delta_{N'_{2e},N_{2e}-1} - \sqrt{(N_{2e}+1)/2}\, \delta_{N'_{2e},N_{2e}+1}]$$

$$\times I_{N_{1h},N'_{1e}}(k_y(\nu)) J_{N_{2h},N'_{2e}} + \frac{\gamma}{B(\nu)} \delta_{N_{1h},N'_{1h}}$$

$$\times I_{N'_{1h},N_{1e}}(k_y(\nu)) J_{N'_{2h},N_{2e}} \left(\sqrt{\frac{N_{2h}+1}{2}}\, \delta_{N_{2h},N'_{2h}-1} \right.$$

$$\left. \left. \left. - \sqrt{\frac{N_{2h}}{2}}\, \delta_{N_{2h},N'_{2h}+1} \right) \right\} \right]^2$$

$$\times \left(\frac{E_g}{\hbar\nu - E_{N_{1e}} - E_{N_{1h}} - E_{N_{2e}} - E_{N_{2h}} - E_g} \right)^{1/2}$$

$$\times |\mathbf{e}_s \cdot \mathbf{Z}|^2, \tag{A16}$$

where

$$\sigma_0 = \frac{e^4 L_y |\mathbf{p}_{cv} \mathbf{e}_l|^2 \hbar^2 n(\nu_s)}{\sqrt{2}\pi m_0^2 m_h^2 E_g^{5/2} n(\nu_l) c^4} \frac{1}{\sqrt{\dfrac{1}{m_e}\left(\dfrac{\omega_{0e}}{\widetilde{\omega}_e}\right)^2 + \dfrac{1}{m_h}\left(\dfrac{\omega_{0h}}{\widetilde{\omega}_h}\right)^2}}, \tag{A17}$$

$$A(\nu) = \frac{\hbar}{E_g}[\nu - \nu_l + (N_{2e} - N'_{2e})\omega_{0e} + (N_{1e} - N'_{1e})\widetilde{\omega}_e], \tag{A18}$$

$$B(\nu) = \frac{\hbar}{E_g}[(N'_{2h} - N_{2h})\omega_{0h} + (N'_{1h} - N_{1h})\widetilde{\omega}_h - \nu + \nu_l], \tag{A19}$$

$$\beta = \frac{m_h}{m_e}, \quad \gamma(H) = \frac{\widetilde{L}_e}{\widetilde{L}_h}, \quad \gamma = \frac{L_e}{L_h}, \tag{A20}$$

and $k_y(\nu)$ is the root of the δ function argument:

$$|k_y(\nu)| = \frac{\sqrt{2}}{\hbar} \sqrt{\frac{\hbar\nu - E_g - E_{N_{1e}} - E_{N_{1h}} - E_{N_{2e}} - E_{N_{2h}}}{\dfrac{1}{m_e}\left(\dfrac{\omega_{0e}}{\widetilde{\omega}_e}\right)^2 + \dfrac{1}{m_h}\left(\dfrac{\omega_{0h}}{\widetilde{\omega}_h}\right)^2}}. \tag{A21}$$

The vectors **X**, **Y**, and **Z** are unit vectors along the corresponding Cartesian axes.

Let us make some remarks concerning the above equations. As indicated above, when $\hbar\nu > E_g$ the Raman process involves the combination of intraband and interband transitions. From Eq. (A12) it follows that $J_{N_{2h}, N'_{2e}}$ ($J_{N'_{2h}, N_{2e}}$) vanishes unless $N_{2h} + N'_{2e} = 2n$ ($N'_{2h} + N_{2e} = 2n$) where n is an integer. So a transition can only take place between N_{2h} and N'_{2e} (N'_{2h} and N_{2e}) subbands with the same parity ($2m \to 2n$ and $2m+1 \to 2n+1$; m and n are integers). But for Eq. (A11) quantum numbers N_{1h} and N'_{1e} (N'_{1h} and N_{1e}) can change arbitrarily.

Hence, the following selection rules are obtained for interband transitions:

$$|N_{1h} - N'_{1e}| = 0, 1, 2, \ldots, \quad |N_{2h} - N'_{2e}| = 0, 2, 4, \ldots,$$

$$|N'_{1h} - N_{1e}| = 0, 1, 2, \ldots, \quad |N'_{2h} - N_{2e}| = 0, 2, 4, \ldots.$$

(i) When $H = 0$, $x_{0e} = x_{0h} = 0$, $\widetilde{L}_e = L_e$, and $\widetilde{L}_h = L_h$, which is the oscillator center of the conduction and valence band electrons coincident. Then, making the replacement $N_{2h} \to N_{1h}, N'_{2e} \to N'_{1e}$ ($N'_{2h} \to N'_{1h}, N_{2e} \to N_{1e}$), we see that Eq. (A11) turns into Eq. (A12). Thus, for $H = 0$ we have the selection rules

$$|N_{1h} - N'_{1e}| = 0, 2, 4, \ldots, \quad |N_{2h} - N'_{2e}| = 0, 2, 4, \ldots,$$

$$|N'_{1h} - N_{1e}| = 0, 2, 4, \ldots, \quad |N'_{2h} - N_{2e}| = 0, 2, 4, \ldots.$$

(ii) The case $\omega_{e(h)} \gg \omega_{0e(h)}$. This condition corresponds to the strong magnetic fields, and we have

$$\widetilde{\omega}_{e(h)} = \omega_{e(h)} \sqrt{1 + \left(\frac{\omega_{0e(h)}}{\omega_{e(h)}}\right)^2} \approx \omega_{e(h)}$$

and

$$x_{0e} \approx x_{oh}, \quad \widetilde{L}_e \approx \widetilde{L}_h = \sqrt{\frac{c\hbar}{eH}} = l_H,$$

where l_H is the magnetic length. For this case Eq. (A11) differs from zero when $N_{1h} = N'_{1e}$ ($N'_{1h} = N_{1e}$). In this way, the

selection rule $|N_{1h} - N'_{1e}| = 2n+1$ ($|N'_{1h} - N_{1e}| = 2n+1$) takes place in intermediate magnetic fields.

As can be seen from Eqs. (A14) and (A16) the differential cross section is directly proportional to the density of states of carriers in the valence and conduction bands and to the interband matrix elements. In this case the scattering spectrum shows density-of-states peaks and interband matrix elements maximums. The positions of these structures are given as follows:

$$\hbar\nu = E_{N_{1h}} + E_{N_{2h}} + E_{N_{1e}} + E_{N_{2e}} + E_g. \tag{A22}$$

Here, the following selection rules must be fulfilled: $N'_{1e} = N_{1e} \pm 1$, $N'_{2e} = N_{2e}$ ($N'_{1h} = N_{1h} \pm 1, N'_{2h} = N_{2h}$) for X scattering configuration and $N'_{2e} = N_{2e} \pm 1$, $N'_{1e} = N_{1e}$ ($N'_{2h} = N_{2h} \pm 1, N'_{1h} = N_{1h}$) for Z scattering configuration. In this case when $|N_{1h} - N'_{1e}| = 2n+1$ ($|N'_{1h} - N_{1e}| = 2n+1$) the spectrum shows maxima and when $|N_{1h} - N'_{1e}| = 2n$ ($|N'_{1h} - N_{1e}| = 2n$) the ERS spectrum shows singular peaks. The peaks and maxima related to these structures correspond to interband EHP transitions and their positions depend on the magnetic field.

Other singularities of Eqs. (A14) and (A16) occur whenever $A(\nu) = 0$ and $B(\nu) = 0$. In the X scattering configuration this singularities are

$$\nu = \nu_l - \widetilde{\omega}_e, \quad \nu = \nu_l - \widetilde{\omega}_h. \tag{A23}$$

Here the following selection rules are fulfilled: $N'_{1e} = N_{1e} + 1$, $N'_{2e} = N_{2e}$ and $N'_{1h} = N_{1h} - 1$, $N'_{2h} = N_{2h}$.

For the Z scattering configuration the Raman singularity is

$$\nu = \nu_l - \omega_{0e}, \quad \nu = \nu_l - \omega_{0h}. \tag{A24}$$

In this case the selection rules are $N'_{1e} = N_{1e}$, $N'_{2e} = N_{2e} + 1$ and $N'_{1h} = N_{1h}$, $N'_{2h} = N_{2h} - 1$.

As can be seen from Eqs. (A23) and (A24) these frequencies correspond to electron transitions connecting the subband edges for a process involving the conduction and valence bands (i.e., intraband transitions). We can also notice that the Y scattering configuration is free from Raman singularities and relates to the selection rules $N'_{1e} = N_{1e}$, $N'_{2e} = N_{2e}$ and $N'_{1h} = N_{1h}$, $N'_{2h} = N_{2h}$.

---

[1] Y. Nagamune, Y. Arakawa, S. Tsukamoto, M. Nishioka, S. Sasaki, and M. Miura, Phys. Rev. Lett. **69**, 2963 (1992).

[2] A. S. Plaut, H. Lage, P. Grambow, D. Heitmann, K. von Klitzing, and K. Ploog, Phys. Rev. Lett. **67**, 1642 (1991).

[3] T. Demel, D. Heitmann, P. Grambow, and K. Ploog, Phys. Rev. Lett. **66**, 2657 (1991).

[4] A. R. Goni, A. Pinczuk, J. S. Weiner, B. S. Dennis, L. N. Pfeiffer, and K. W. West, Phys. Rev. Lett. **70**, 1151 (1993).

[5] K. K. Choi, D. C. Tsui, and S. C. Palmateer, Phys. Rev. B **33**, 8216 (1986).

[6] C. J. B. Ford, T. J. Thornton, R. Newbery, M. Pepper, H. Ahmed, G. Davies, and D. Andrews, Superlattices Microstruct. **4**, 451 (1988).

[7] J. Liu, K. Ismail, K. Y. Lee, J. M. Hong, and S. Washburn, Phys. Rev. B **47**, 13039 (1993).

[8] J. A. Brum, G. Bastard, L. L. Chang, and L. Esaki, Superlattices Microstruct. **3**, 47 (1987).

[9] G. Bastard, J. A. Brum, and R. Ferreira, Semicond. Sci. Technol. **44**, 395 (1991).

[10] A. Lorenzoni and L. C. Andreani, Semicond. Sci. Technol. **14**, 1169 (1999).

[11] M. Cardona and G. Güntherodt, in *Light Scattering in Solids V*, Topics in Applied Physics, Vol. 66 (Springer, Heidelberg, 1989).

[12] M. Cardona, Superlattices Microstruct. **7**, 183 (1990).

[13] F. Comas, C. Trallero-Giner, and R. J. Perez-Alvarez, J. Phys. C **19**, 6479 (1986).

[14] A. Pinczuk and E. Burstein, in *Light Scattering in Solids I*, Springer Topics in Applied Physics, Vol. 8, edited by M. Cardona (Springer, Heidelberg, 1983).

[15] R. F. Wallis and D. L. Mills, Phys. Rev. B **2**, 3312 (1970).

[16] F. Comas, C. Trallero-Giner, I. G. Lang, and S. T. Pavlov, Fiz. Tverd. Tela (Leningrad) **27**, 57 (1985) [Sov. Phys. Solid State **27**, 32 (1985)].

[17] F. Bechstedt, R. Enderlein, and K. Peuker, Phys. Status Solidi B **68**, 43 (1975).

[18] R. Riera, F. Comas, C. Trallero-Giner, and S. T. Pavlov, Phys. Status Solidi B **148**, 533 (1988).

[19] R. Betancourt-Riera, J. M. Bergues, R. Riera, and J. L. Marin, Physica E (Amsterdam) **5**, 204 (2000).

[20] J. H. Burnett, H. M. Cheong, R. M. Westervelt, W. Paul, P. F. Hopkins, M. Sundaram, and A. C. R. Cossard, Phys. Rev. B **48**, 4524 (1993).

[21] R. C. Miller, D. A. Kleinman, and A. C. Gossard, Phys. Rev. B **29**, R7085 (1984).

[22] J. Batey, S. L. Wright, and D. J. Di Maria, J. Appl. Phys. **57**, 484 (1985).